Cancer Science
Japanese Cancer Association JCA
Open Access

Epigenetic deregulation of *Ellis Van Creveld* confers robust Hedgehog signaling in adult T-cell leukemia

Ryutaro Takahashi,[1,6] Makoto Yamagishi,[1,6] Kazumi Nakano,[1] Toshiko Yamochi,[2] Tadanori Yamochi,[1] Dai Fujikawa,[1] Makoto Nakashima,[1] Yuetsu Tanaka,[3] Kaoru Uchimaru,[4] Atae Utsunomiya[5] and Toshiki Watanabe[1]

[1]Graduate School of Frontier Sciences, The University of Tokyo, Tokyo; [2]Department of Pathology, Showa University School of Medicine, Tokyo; [3]Department of Immunology, Graduate School of Medicine, University of the Ryukyus, Okinawa; [4]Institute of Medical Science, The University of Tokyo, Tokyo; [5]Department of Hematology, Imamura Bun-in Hospital, Kagoshima, Japan

Key words

ATL, epigenetics, EVC, Hedgehog, HTLV-1

Correspondence

Toshiki Watanabe, Laboratory of Tumor Cell Biology, Department of Medical Genome Sciences, Graduate School of Frontier Sciences, The University of Tokyo, 4-6-1 Shirokanedai, Minato-ku, Tokyo 108-8639, Japan.
Tel: +81-3-5449-5298; Fax: +81-3-5449-5418;
E-mail: tnabe@ims.u-tokyo.ac.jp

[6]These authors contributed equally to this study.

Funding information

JSPS KAKENHI (24790436). (23390250). MEXT KAKENHI (221S0001). Ministry of Health, Labour and Welfare H24-Third Term Cancer-004 Uehara Memorial Foundation.

Received April 14, 2014; Revised June 20, 2014; Accepted July 1, 2014

Cancer Sci **105** (2014) 1160–1169

doi: 10.1111/cas.12480

One of the hallmarks of cancer, global gene expression alteration, is closely associated with the development and malignant characteristics associated with adult T-cell leukemia (ATL) as well as other cancers. Here, we show that aberrant overexpression of the *Ellis Van Creveld* (EVC) family is responsible for cellular Hedgehog (HH) activation, which provides the pro-survival ability of ATL cells. Using microarray, quantitative RT-PCR and immunohistochemistry we have demonstrated that EVC is significantly upregulated in ATL and human T-cell leukemia virus type I (HTLV-1)-infected cells. Epigenetic marks, including histone H3 acetylation and Lys4 trimethylation, are specifically accumulated at the *EVC* locus in ATL samples. The HTLV-1 Tax participates in the coordination of EVC expression in an epigenetic fashion. The treatment of shRNA targeting EVC, as well as the transcription factors for HH signaling, diminishes the HH activation and leads to apoptotic death in ATL cell lines. We also showed that a HH signaling inhibitor, GANT61, induces strong apoptosis in the established ATL cell lines and patient-derived primary ATL cells. Therefore, our data indicate that HH activation is involved in the regulation of leukemic cell survival. The epigenetically deregulated EVC appears to play an important role for HH activation. The possible use of EVC as a specific cell marker and a novel drug target for HTLV-1-infected T-cells is implicated by these findings. The HH inhibitors are suggested as drug candidates for ATL therapy. Our findings also suggest chromatin rearrangement associated with active histone markers in ATL.

Adult T-cell leukemia (ATL) is a malignant T-cell disorder caused by infection with a human retrovirus, human T-cell leukemia virus type I (HTLV-1).[1–3] The prognosis of aggressive types of ATL is poor.[4] At present, ATL is an intractable disease in human beings. To prevent the development of ATL and the poor prognosis that is associated with it, the development of effective therapies based on the molecular characteristics is needed.

To explore effective drugs, precise understanding of the molecular mechanism of ATL pathogenesis is essential. We have previously reported that genetic and epigenetic imbalances and following aberrant gene expressions are the main framework for ATL tumor cells.[5,6] In addition, the involvement of systemic downregulation of cellular microRNA has been implicated in the leukemogenesis of ATL. So far, several host cellular signaling abnormalities induced by HTLV-1 Tax in the early phase of infection[6–8] and the aberrant activation of nuclear factor-kappa B (NF-κB) contribute to ATL leukemogenesis.[9,10] Although other several molecular deregulations have been suggested in ATL, we have not completely covered the landscape of signaling networks in ATL.

Recently, Hedgehog (HH) signaling has been reported as an oncogenic pathway in many types of cancers.[11,12] Constitutive HH activation leads to the overproliferation or survival of several cancer cells, such as basal cell carcinoma or B-cell lymphomas.[13–15] There are some HH inhibitors under clinical trial as drug candidates against those cancers.[16]

In the present study, using ATL patient samples and some ATL models, we found two specific gene overproductions in ATL, *Ellis Van Creveld syndrome 1* (*EVC1*) and *EVC2*, which belong to the EVC family of genes that are implicated in HH regulation.[17–19] We demonstrated that epigenetically upregulated EVC was associated with cellular HH activity. *EVC* and other regulatory factors for HH signaling were responsible for the survival of ATL cell lines and also primary ATL samples. Direct evidence from the ATL samples revealed that universal epigenetic marks associated with actively transcribed genes were rearranged in the leukemic cells. These findings may shed light on the abnormal gene expression signature and leukemic cell traits observed in ATL.

Materials and Methods

Patient samples. The primary peripheral blood mononuclear cells (PBMC) from ATL patients and healthy volunteers were a part of those collected with informed consent as a collaborative project of the Joint Study on Prognostic Factors of ATL Development (JSPFAD). The project was approved by the University

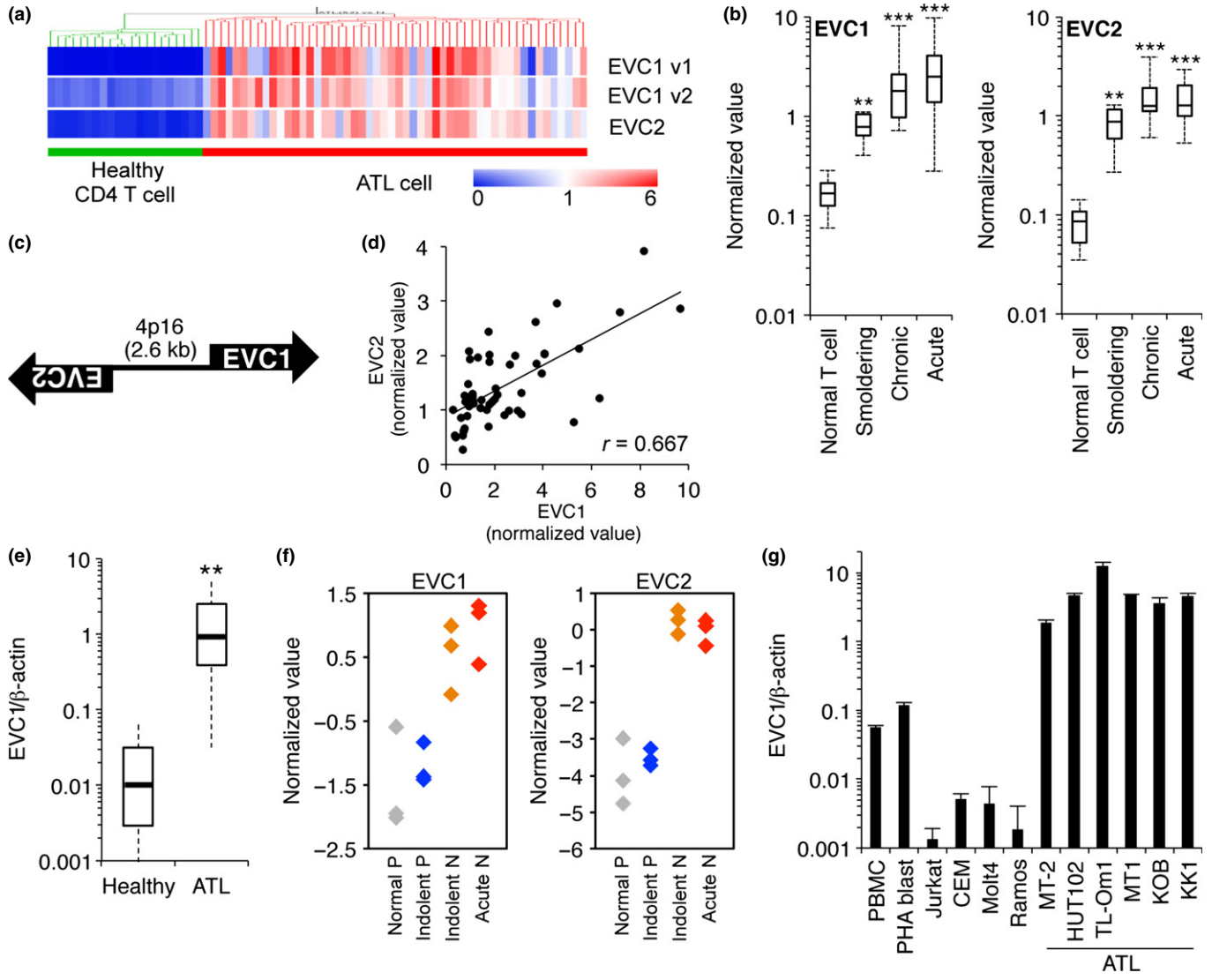

Fig. 1. *EVC* overexpression in ATL. (a, b) Microarray heatmap (a) and box plot (b) of *EVC*. $^{**}P < 0.01$. $^{***}P < 0.001$. (c) Schematic illustration of locus encoding *EVC1/2*. (d) Individual expression values ($n = 52$) between *EVC1* and *EVC2*. (e) *EVC1* mRNA level in ATL patient PBMC (total, $n = 11$; acute, $n = 7$; chronic, $n = 4$) and in CD4+ T cells from healthy donors ($n = 6$) evaluated using quantitative RT-PCR (qRT-PCR). $^{**}P < 0.01$. (f) *EVC1* and *EVC2* levels in CADM1 versus CD7 plot subpopulations. Normal P, CD4+/CADM1−/CD7+ T cells from healthy donors; Indolent P, CD4+/CADM1−/CD7+ from indolent ATL patients; Indolent N, CD4+/CADM1+/CD7− from indolent ATL patients; Acute N, CD4+/CADM1+/CD7− from acute ATL patients. The gene expression microarray dataset is available in Kobayashi *et al.*[25] (g) *EVC1* levels in various cell lines examined using qRT-PCR ($n = 3$, mean ± SD).

of Tokyo and Showa University research ethics committees. The PBMC were isolated using Ficoll separation and maintained in RPMI1640 (Invitrogen, Carlsbad, CA, USA) supplemented with 1% of self-serum and antibiotics (Invitrogen). Clinical information is shown in the Supporting Information Methods.

Microarray analysis. Gene expression profiling of ATL patient samples and normal CD4+ T cells has been performed previously.[5] The coordinate has been deposited in the Gene Expression Omnibus database (GSE33615).

Cell culture. The HTLV-1-infected cell lines MT-2 and HUT102, ATL-derived cells MT-1 and TL-Om1, and other leukemic cell lines were cultured in RPMI1640 with 10% FCS. ATL-derived KOB and KK1 were cultured in RPMI1640 with 10% FCS and 10 ng/mL recombinant human IL-2 (R&D Systems, Minneapolis, MN, USA). The 293T cell was cultured in DMEM with 10% FCS. All cell lines were cultured at 37°C, with 5% CO_2.

Plasmids and HH activity analysis. Tax-encoding plasmids have been described previously.[20] *EVC1* cDNA was amplified as two fragments from the human cDNA library. Cellular HH activity was evaluated using a dual-luciferase assay (Promega, Madison, WI, USA).[21] Briefly, 7 × GLI binding site (GACACCCA)-luciferase plasmid and control RSV-Renilla plasmid were co-transfected into target cells using Lipofectamine2000 (Invitrogen). At 24 h post-transfection, the cells were collected and analyzed using a dual-luciferase assay.

Quantitative RT-PCR. Procedures for RNA isolation and RT-PCR have been described previously.[5] Primer sets for quantitative RT-PCR (qRT-PCR) are provided in the Supporting Information Methods.

Epigenetic analyses. Bisulfite treatment was conducted using a MethylEasy Xceed Rapid DNA Bisulphite Modification kit (Human Genetic Signatures, NSW, Australia). For evaluating histone covalent modifications, a chromatin immunoprecipita-

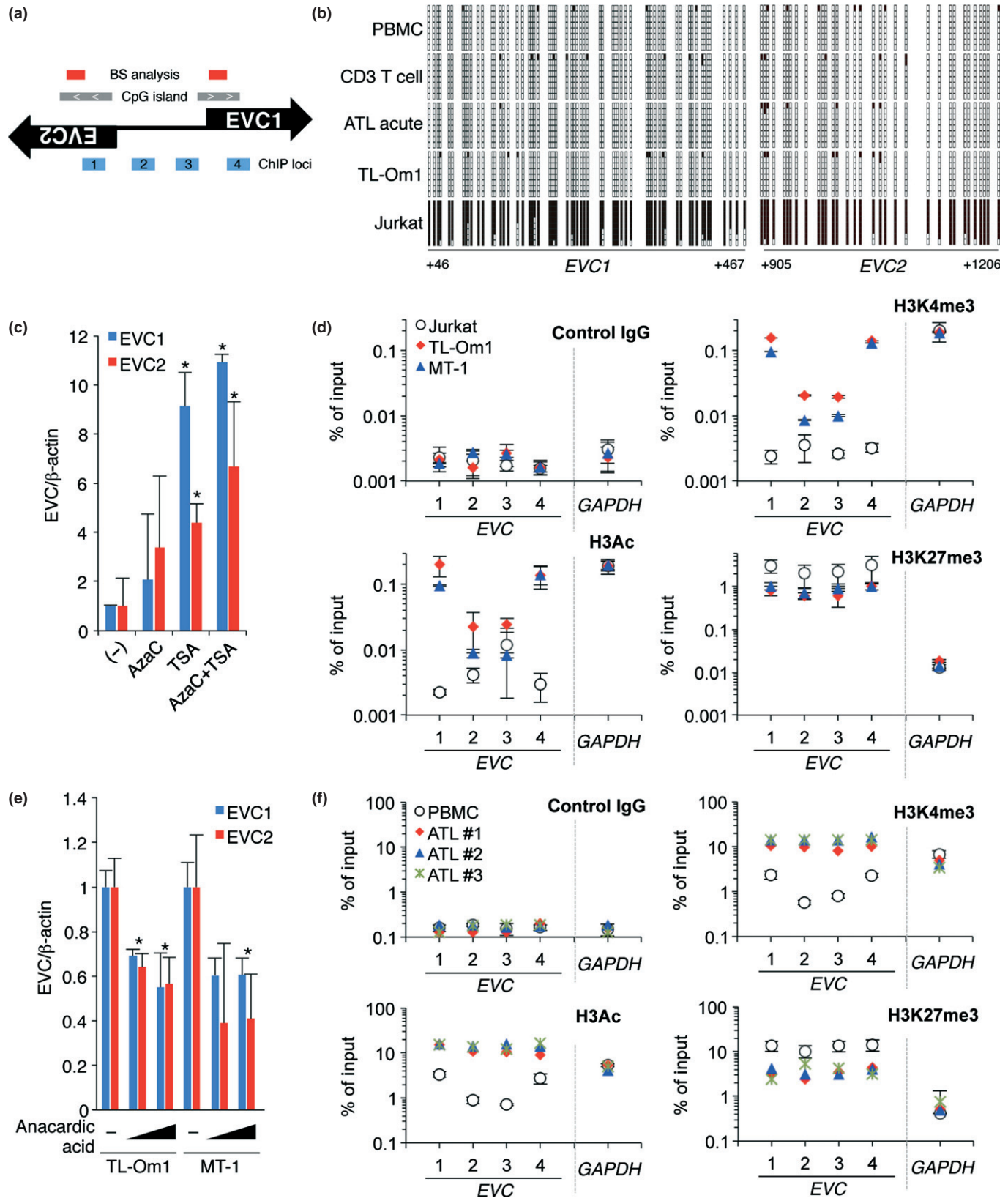

Fig. 2. Epigenetic reprogramming in the *EVC* locus. (a) Schematic of CpG islands and chromatin immunoprecipitation (ChIP) loci. (b) Results of bisulfite sequencing (+46 to +466 from *EVC1* transcription start site [TSS]; +905 to +1206 from *EVC2* TSS). The black and empty boxes represent methylated and unmethylated CpG, respectively. (c) *EVC* RNA levels in Jurkat cells in the presence or absence of epigenetic drugs ($n = 3$, mean ± SD). *$P < 0.05$. (d) Histone covalent modifications at *EVC* and *GAPDH* loci in three cell lines were analyzed using PCR-based ChIP assay with specific antibodies. Positions of primer sets for the real-time PCR are indicated in (a). Enrichment values relative to input samples are plotted. (e) TL-Om1 and MT-1 cells were treated with 1 or 5 μM of anacardic acid for 48 h and the *EVC* mRNA level was then analyzed ($n = 3$, mean ± SD). *$P < 0.05$. (f) Epigenetic changes in primary ATL samples. Three independent clinical samples were compared with normal PBMC ($n = 3$, mean ± SD).

tion (ChIP) assay was conducted as described previously.[5,22] Anti-H3K4me3 (#9751S; Cell Signaling, Danvers, MA, USA), anti-AcH3 (#06-599; Millipore, Billerica, MA, USA), anti-H3K27me3 (#39155; Active Motif, Carlsbad, CA, USA) and control IgG (I5381; SIGMA, St. Louis, MO, USA) were used for ChIP. Primers for the qPCR are provided in the Supporting Information Methods.

Immunohistochemistry. For preparation of the paraffin block of 293T cells, the cells were fixed in 20% of formalin/PBS for 24 h. After removing the formalin, alcohol dehydration and paraffin permeation were done using Tissue-Tek VIP5Jr (Sakura, Alphen aan den Rijn, The Netherlands). Paraffin blocks were sectioned at 3-μm thickness. The sections were then transferred to coating slide glasses (Muto pure chemicals, Bunkyo-ku, Tokyo, Japan). After paraffin removal, the paraffin sections of the 293T and ATL cells were treated with 3% H_2O_2. Antigen-retrieval treatment was done using Histofine antigen retrieval solution pH9 (Nichirei, Chuo-Ku, Tokyo, Japan) for 20 min under microwave radiation. After reaction with the first antibody, anti-EVC antibody (HPA008703, 1:400; SIGMA), and the second antibody (K5027, ENVISION Kit/HRP [DAB]; Dako, Bunkyo-ku, Tokyo, Japan), the sections were colored using ENVISION Kit/HRP [DAB] DAB+ (K3468; DAKO). Finally, the sections were stained with hematoxylin.

Lentivirus construction and production. Detailed procedures for lentivirus production have been described previously.[5] Briefly, replication-defective, self-inactivating lentivirus vectors were used.[23,24] shRNA were cloned into a CS-H1-EVBsd. High-titer viral solutions prepared using a centrifugation-based concentration were transduced into ATL cell lines using the spinoculation method. The transduced cells were

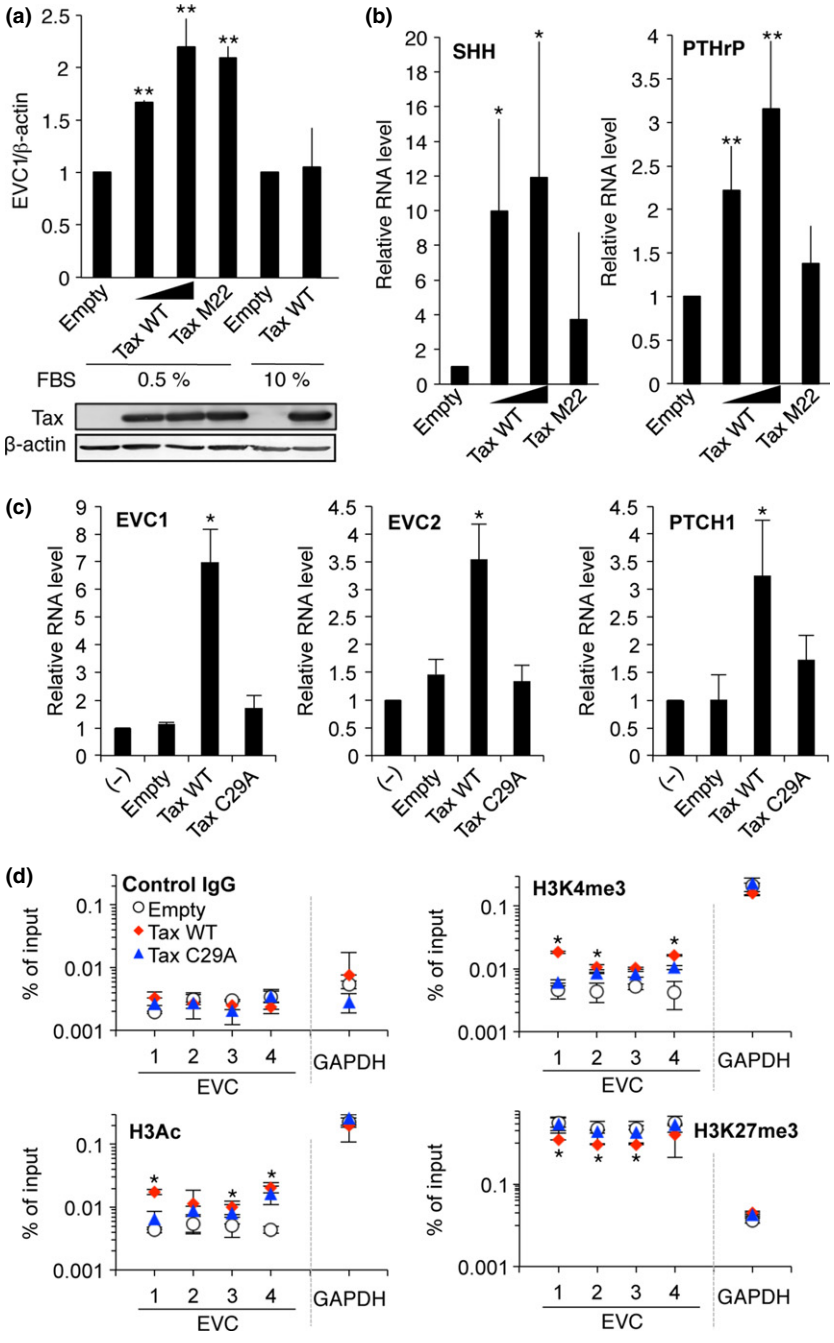

Fig. 3. Role of Tax in *EVC* regulation. (a) *EVC1* RNA levels are affected by Tax. The 293T cells in different FBS condition were transfected with the indicated plasmids. Relative *EVC1* levels were evaluated using quantitative RT-PCR (qRT-PCR) (top panel, $n = 3$, mean ± SD). $^{**}P < 0.01$. Tax expression was confir-med using western blotting with an anti-Tax antibody (Lt-4) (bottom panel). (b) Levels of *SHH* and *PTHrP* in the presence or absence of Tax ($n = 3$, mean ± SD). $^{*}P < 0.05$. $^{**}P < 0.01$. (c) *EVC* and *PTCH1* levels in Jurkat cells expressing Tax ($n = 3$, mean ± SD). $^{*}P < 0.05$. (d) Tax-mediated epigenetic changes. Histone modifications at *EVC* and *GAPDH* loci in Tax-expressing Jurkat cells were analyzed using a ChIP assay. $^{*}P < 0.05$ (Tax WT *vs* Empty). Primer positions are shown in Figure 2(a).

further selected by blastcidin and used within 14 days. shRNA sequences are described in the Supporting Information Methods.

Cell viability and apoptosis analyses. For the cell proliferation assay, 5000 cells were plated in a 96-well flat bottom plate with RPMI1640 medium supplemented with 1% FCS. After 1–3 days culture, cell numbers were evaluated using Cell Counting kit-8 (Dojindo, Kumamoto, Japan). The apoptosis cell was determined using PE Annexin V/7-AAD stainings (BD Pharmingen, San Jose, CA, USA). Detection of apoptotic cells was performed using FACSCalibur (Becton, Dickinson, Franklin Lakes, NJ, USA). Primary ATL cells were defined using sequential gating based on a Forward scatter/Side Scatter (FSC/SSC) pattern and a CD4-positive population (anti-CD4-FITC; BD Pharmingen). Collected data were analyzed using FlowJo software (Tree Star, Ashland, OR, USA).

Results

Epigenetic abnormalities in *EVC* regulation in ATL. We have determined the gene expression signature of ATL tumor cells by conducting massive microarrays.[5] The gene expression profiles from 52 ATL patients and 21 healthy donors identified a large number of specific gene upregulations in ATL cells. Among these, the genes encoding EVC1 and EVC2 were strikingly overexpressed in ATL patient samples, which had a relationship to disease progression (Fig. 1a,b). These genes are located in an identical chromosome *4p16*, under a bi-directional promoter (Fig. 1c), and their expressions have shown a strong positive correlation (Fig. 1d). The qRT-PCR revealed that the median of the *EVC1* mRNA level in ATL was 90.9-fold higher than that of normal CD4+ T-cells (Fig. 1e). Specificity of tumor-associated EVC expression was confirmed using the dataset from CADM1 versus CD7 plot subpopulation samples.[25] CADM1 expression and CD7 loss have recently been identified as highly sensitive molecular markers of HTLV-1-infected cells. *EVC1* and *EVC2* were significantly expressed in the CADM1+/CD7− tumorous population (Fig. 1f). The HTLV-1-infected and ATL-derived cells showed higher levels of *EVC1* mRNA compared with those in other leukemia and lymphoma cell lines and those of healthy PBMC (Fig. 1g). The MT-2 and HUT102 cells, which highly express HTLV-1 genes, showed high *EVC1* mRNA levels similar to those in ATL-derived cells.

Looking at the tumor-associated epigenetic reprogramming that was frequently observed in ATL,[5,6] we analyzed the epigenetic status of the *EVC* locus to clarify the possible

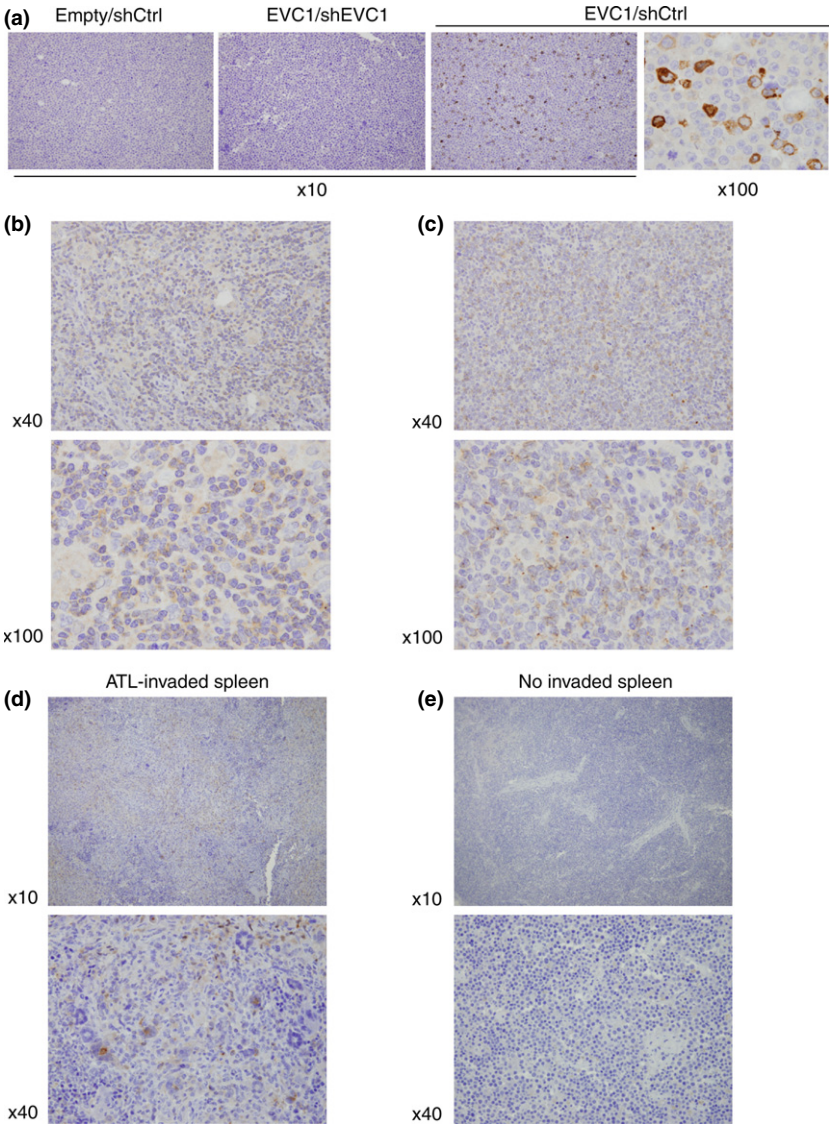

Fig. 4. EVC1 expression in ATL cells. (a–e) Immunohistochemistry-based EVC1 protein detection in paraffin-embedded samples: 293T transfected with the indicated plasmids (a), primary ATL lymph node (b, c, representative data are shown) and spleen from mice engrafted with primary ATL cells (d, tumor invasive, $n = 3$; e, non-invasive). These samples were stained with anti-EVC1 antibody and hematoxylin.

involvement of epigenetic variation in *EVC* deregulation. There were two typical CpG islands in the *EVC* locus whose transcription may be tightly regulated by the gain of CpG methylation (Fig. 2a). However, bisulfite sequencing revealed that DNA methylation was not acquired in normal lymphocytes, as well as in the primary ATL sample (Fig. 2b). CpG hypermethylation within the *EVC* locus was found only in Jurkat cells where the *EVC* expression was nearly undetectable (Fig. 1g). Instead, treatment with epigenetic drugs, particularly a histone deacetylase (HDAC) inhibitor tricostatin A (TSA), reactivated the *EVC* transcription in Jurkat cells, suggesting that histone modifications such as acetylation were involved in *EVC* regulation (Fig. 2c). To further address the epigenetic implication, we performed ChIP assays to assess the possible contribution of histone modification in *EVC* upregulation. The ATL cell lines showed significant accumulation (log-scale) of histone H3 acetylation (H3Ac) and H3K4 trimethylation (H3K4me3), which have been recognized generally as positive transcription marks around the transcription start site region of both *EVC1* and *EVC2* (Fig. 2d). Treatment with a pan-histone acetylase inhibitor, anacardic acid, reduced *EVC* transcription in ATL cell lines (Fig. 2e). Interestingly, H3K27me3, which has been implicated as a poor prognostic marker in ATL,[5,26] was decreased at the *EVC* locus in ATL cells. We confirmed directly the epigenetic reprogramming at the *EVC* locus in primary ATL samples (Fig. 2f). In summary, it appeared that the acquisition of active histone modifications and the reciprocal disappearance of H3K27me3 contributed to aberrant EVC transcription.

Role of HTLV-1 Tax in *EVC* transcription. Next we addressed whether Tax could participate in the deregulated *EVC1* transcription. Although Tax expression did not influence the *EVC1* mRNA levels in 293T cells at complete growth conditions, Tax activated *EVC1* transcription in a dose-dependent manner in serum-starved conditions (Fig. 3a). A NF-κB activation-defected Tax mutant, M22,[27] showed similar *EVC1* induction, suggesting that *EVC1* transcriptional activation was independent from NF-κB activation. Indeed, the pharmacological inhibition of NF-κB activity failed to prevent *EVC* transcription in ATL cell lines (data not shown). Meanwhile, Tax induced transcription of *Sonic hedgehog* (*Shh*), which encodes the HH activation ligand, in a NF-κB-dependent manner (Fig. 3b). The experimental condition was validated by the evaluation of *PTHrP*, which has been known to be a Tax and NF-κB-targeted gene. HTLV-1 *HBZ* did not affect *EVC* transcription (Supporting Information Fig. S1).

We examined the possible relationship between Tax and histone modifications. For this purpose, we established lentiviral vectors inducing stable Tax expression in Jurkat cells. More than 80% of transduction efficiencies were achieved in all tested cells. Tax induced transcription of *EVC1* and *EVC2*, as well as the HH target gene *PTCH1* (Fig. 3c). Interestingly, the Tax C29A mutant, which was unable to localize in the nucleus,[28] failed to induce *EVC*, suggesting that *EVC* induction was directly caused by the nuclear-localized Tax. A ChIP assay revealed that the Tax wild type, but not the C29A mutant, directly accumulated H3K4me3 and H3Ac in the *EVC* locus (Fig. 3d). Thus, Tax appeared to, at least partially, induce *EVC* expression through epigenetic reprogramming.

EVC1 expression in primary ATL cell. We performed immunohistochemistry (IHC) with a commercially available antibody that recognized EVC1. First, we stained paraffin-embedded 293T cells transduced with the EVC1-expressing plasmid to test the antibody specificity. Strong positivity was detected in the plasmid-transduced sample but not in samples with untreated or concomitantly treated with shRNA targeting *EVC1* (Fig. 4a). Using this antibody we investigated EVC1 expression in several aggressive ATL cases. Most ATL cases showed stable EVC1 positivity (7/8, 87.5%; two representatives in Fig. 4b,c). We noted that all EVC1-positive cells were dysplastic. Furthermore, EVC1 expression was clearly detected in a mouse ATL model that was established using xenotrans-

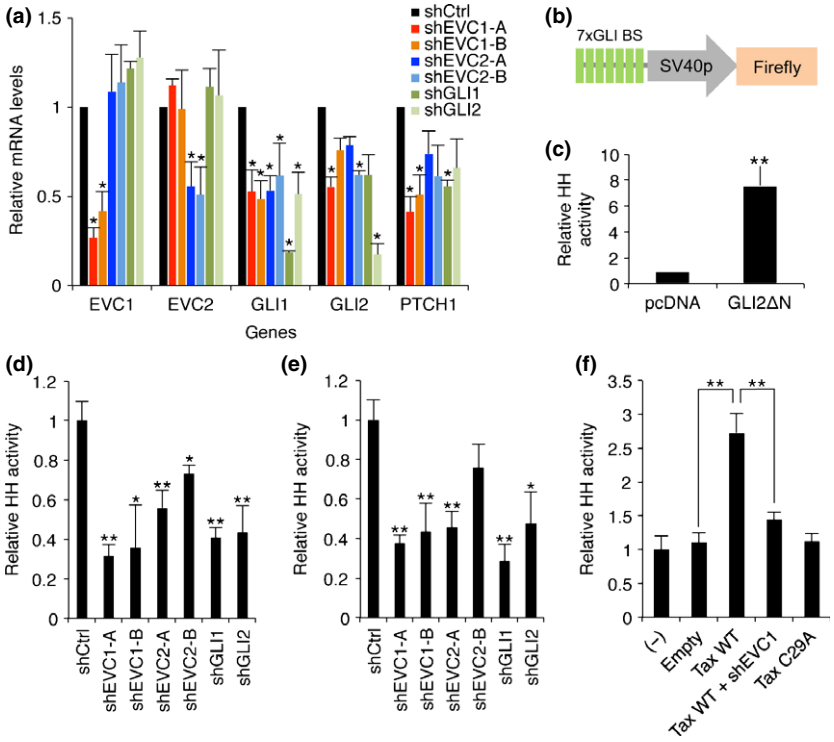

Fig. 5. EVC supports Hedgehog (HH) activity. (a) Relative RNA levels in shRNA-expressing TL-Om1 cells ($n = 3$, mean ± SD). $^{*}P < 0.05$. (b) Luciferase reporter plasmid containing 7 × sequential GLI-binding sites. (c) GLI2ΔN activa-ted HH activity ($n = 3$, mean ± SD). $^{**}P < 0.01$. (d–f) Hedgehog activity in various shRNA-expressing TL-Om1 (d), MT-2 (e) and Tax and shEVC1-expressing Jurkat (f) ($n = 3$–4, mean ± SD). $^{*}P < 0.05$. $^{**}P < 0.01$.

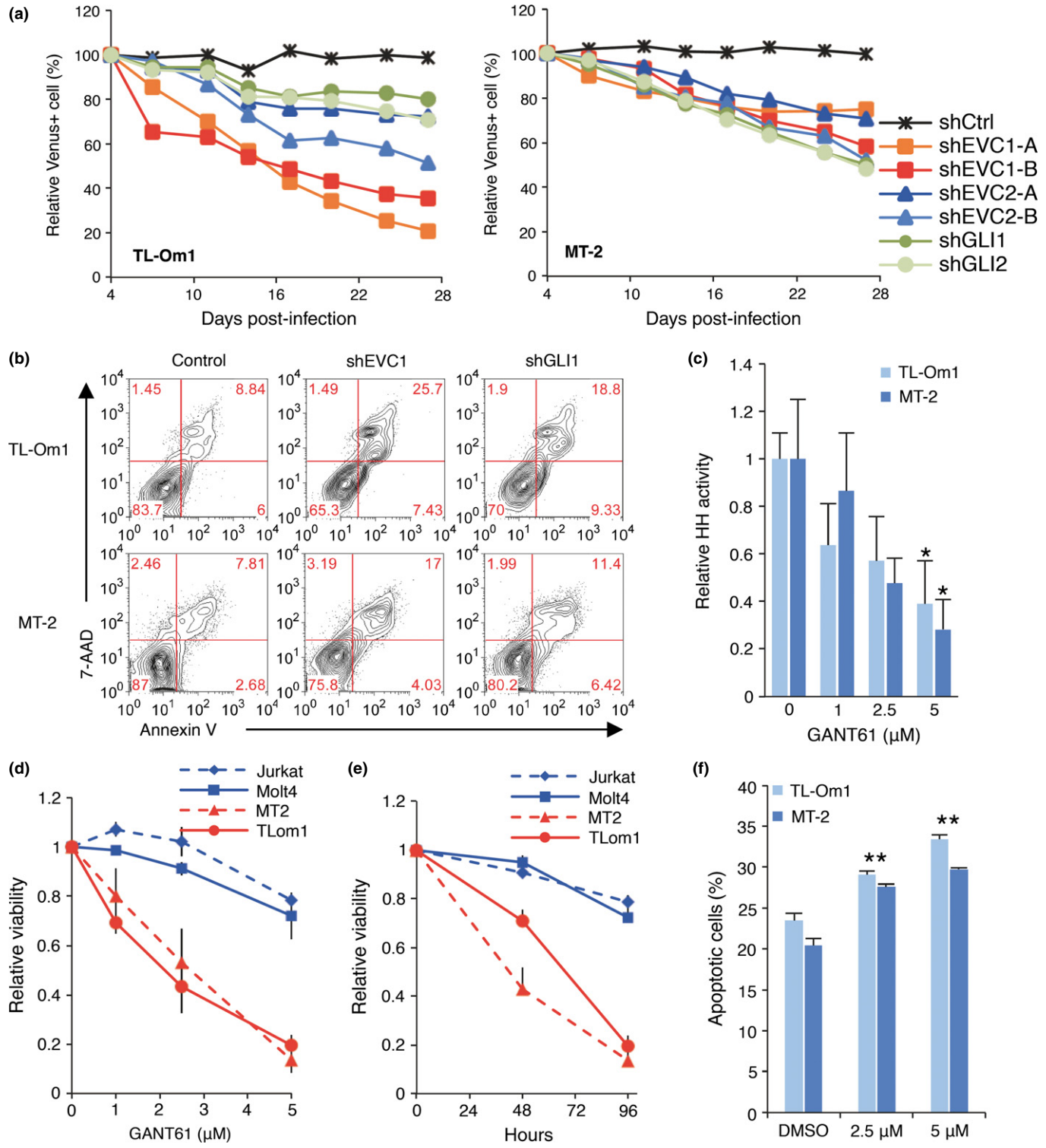

Fig. 6. Hedgehog (HH)-dependent ATL cell survival. (a) Time course of the abundance of Venus+ TL-Om1 (left) and MT-2 (right) infected with lentiviral vector expressing control shRNA (shCtrl), either of two shRNA targeting EVC1 and EVC2, or shRNA targeting GLI1 and GLI2, then cultured for 27 days together with uninfected cells. Data are representative of three independent experiments. Results are presented relative to those of cells at 4 days post-infection. (b) shRNA-mediated apoptosis induction. shRNA-expressing cells were cultured in 1% FBS for 72 h. The apoptotic pattern was defined by gating with Venus+ and Annexin V/7-AAD ($n = 3$, representative data). (c) GANT61 inhibited HH activity in ATL cells ($n = 3$, mean ± SD). $^*P < 0.05$. (d–e) GANT61 reduced ATL cell viability ($n = 3$, mean ± SD). The cells were treated with the indicated concentrations of GANT61 for 96 h (d) or with 5 μM of GANT61 for the indicated time periods (e). Cells were maintained in 1% FCS. (f) GANT61-dependent apoptosis analyzed using Annexin V/7-AAD staining ($n = 3$, mean ± SD). $^{**}P < 0.01$.

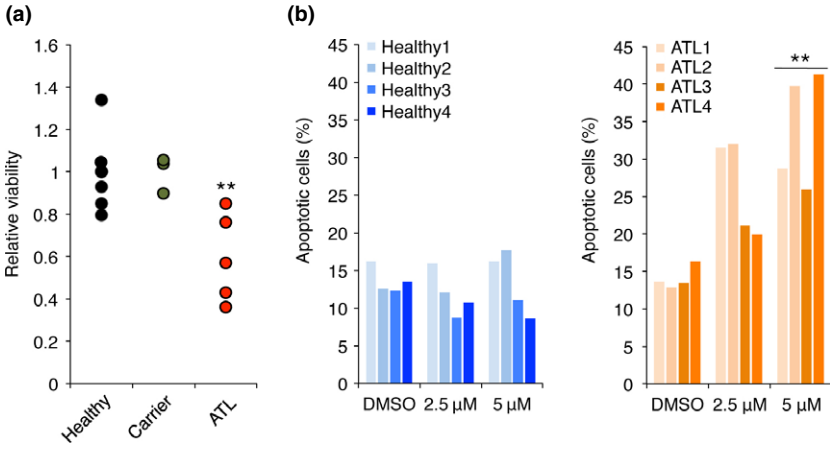

Fig. 7. GANT61 treatment reduced cell viabilities of primary ATL samples. (a) Effect of GANT61 in primary PBMC samples. The PBMC from healthy donors ($n = 7$), asymptomatic carriers ($n = 3$) and ATL patients ($n = 5$) were exposed in 5 μM of GANT61 for 72 h. Cells were maintained in media with 1% self-serum. $^{**}P < 0.01$. (b) GANT61-dependent apoptosis in ATL samples. The PBMC from healthy donors ($n = 4$) and ATL patients ($n = 4$) were treated with 5 μM of GANT61 for 72 h. Graphs show percentiles of apoptotic population in CD4+ cells $^{**}P < 0.01$.

plantation of primary tumor cells derived from an ATL patient. The lymphoma cells specifically expressed EVC1 (Fig. 4d,e). Taken together, EVC1 protein was definitely expressed in ATL cells.

EVC in HH activation. The EVC family has been implicated in HH signaling.[18,19] We performed the knockdown of EVC in TL-Om1 and MT-2 cells, which all highly expressed EVC (Fig. 1g). Specific knockdown was accomplished using lentivirus harboring specific and previously validated shRNA against EVC1, EVC2 or GLI transcription factors in the HH cascade. The qRT-PCR revealed the knockdown efficiency and also the HH activity as the RNA levels of *PTCH1* and *GLI1* were well-established HH activity markers.[29] The EVC depletion resulted in reduction of *PTCH1* and *GLI1* mRNA levels (Fig. 5a). Next we established a luciferase reporter containing 7 × sequential GLI-binding sites (Fig. 5b), which strongly responded against GLI2ΔN, a constitutive active form of GLI2[12] (Fig. 5c). As expected, the knockdown of EVC1 and EVC2 represented diminished HH activity in TL-Om1 and MT-2 cells (Fig. 5d,e). In addition, Tax activated the HH signal in Jurkat cells (Fig. 5f). Knockdown of EVC1 cancelled Tax-directed HH activation, suggesting that Tax affects HH signaling through, at least partially, EVC induction epigenetically.

EVC-dependent cell survival in ATL. Aberrant activation of HH provides cell survival ability in myeloma and lymphoma.[14,15] We found that different shRNA targeting EVC and GLI caused a progressive depletion of Venus+ cells (Fig. 6a). Knockdown of EVC1 or EVC2 attenuated ATL cell proliferation (Fig. S2). The growth defect was associated with a substantial decrease in the expression of targeted genes (Fig. 5). We then measured the apoptotic status by staining Annexin V/7-AAD. Specific analyses within the knocked down cells were achieved by gating with Venus fluorescence. At complete growth condition, slight but steady apoptosis was induced by EVC1 knockdown in MT-2 and TL-Om1 cells (data not shown). Furthermore, strong apoptosis was observed in EVC1-depleted cells at low FCS condition (Fig. 6b). This cell death appeared to be due to HH inactivation because GLI1-knocked down cells showed similar results.

Specific killing of ATL cell by GANT61. GANT61 is a cell-permeable hexahydropyrimidine compound, which has been shown to be a well-established inhibitor of GLI-mediated gene transactivation.[29] GANT61 treatment successfully reduced GLI binding to the target sequence (Fig. 6c). In that condition, MT-2 and TL-Om1 cells showed remarkable reduction of cell viability by GANT61 treatment in dose- and time-dependent manners (Fig. 6d,e), which may be caused by apoptosis (Fig. 6f).

Finally, we evaluated the pharmacological activity of GANT61 on primary ATL samples. Although GANT61 did not show a clear effect on PBMC derived from healthy donors and HTLV-1 carriers, its treatment specifically reduced the viability of ATL samples significantly (Fig. 7a). Flow cytometry demonstrated that GANT61 specifically killed CD4+ leukemic cells from ATL patients via apoptosis induction (Fig. 7b).

Discussion

A large number of efforts have collectively concluded that aberrant gene expression patterns contribute to the malignant characteristics in ATL and other neoplastic cells. In the present study, based on the careful analyses of patient samples, we have demonstrated that *EVC* is drastically overexpressed in mRNA and its protein can be specifically detected in ATL cells in contrast to normal CD4+ T-cells. To the best of our knowledge, this is the first report regarding EVC expression and function in lymphocytes. The results of the microarray indicate that *EVC* expression appears to be induced in accordance with disease progression. EVC1 protein expression is observed in dysplastic ATL cells derived from patients and a xenotransplantation model. Because the EVC family may be membrane-associated proteins (Fig. 4),[30] the present study provides us with the possibility that EVC expressions might be useful cell markers of HTLV-1-infected T-cells for future clinical purposes.

The EVC family has been identified initially as the responsible genes for one morphogenic disorder, Ellis van Creveld syndrome; it is also believed to play a role in the determination of body-axis or morphogenesis by usually bearing one step of the HH signaling pathway.[12,17–19] Knockout studies have demonstrated that EVC1 and EVC2 cooperatively act as positive modulators of the HH pathway in mouse fibroblasts and chondrocytes. However, abnormal EVC upregulation has not been reported in any cancers; whether the HH pathway is sensitive to cellular dynamism of EVC has not been elucidated as yet. Herein, we demonstrated that overexpression of EVC can be linked to HH activity in T cells for the first time. In addition, several experimental results, including the knockdown assay and GANT61 treatment, suggest totally that the HH pathway was activated in ATL, which in turn contributed to ATL cell survival. Further study will be required for mechanistic insights on how EVC activates HH in T cells.

Further investigation uncovered that transcription from the *EVC* locus was coordinated by epigenetic alteration. In particular, the lymphoma-associated H3Ac and H3K4me3 accumulations appeared to dominate EVC upregulation. Direct evidence from patient samples supported the epigenetic reprogramming, including previously unappreciated H3K4me3 rearrangements, conferring robust EVC expression. Interestingly, repressive histone mark H3K27me3 was mutually reduced at the *EVC* locus in the ATL samples, suggesting that cooperative regulation in this bivalent domain may define the EVC expression and possibly HH activity.

HTLV-1 Tax was involved in the regulation of EVC via epigenetic regulation. Nuclear localization-deficient Tax mutant was unable to induce EVC expression, implying that Tax may participate directly in determination of chromatin architecture. Indeed, lentiviral expression of Tax partially increased active histone modifications, which in turn activated HH signaling. Previously, we and others have reported that Tax physically binds with histone modifying factors, including HDAC,[31] SUV39H1[32] and SMYD3.[20] Interplay between Tax and epigenetic rearrangement may be closely involved in the progression of HTLV-1-infected cells to leukemic cells. Meanwhile, other ATL-specific epigenetic events including significant modifications on histone acetylation, H3K4me3 and H3K27me3 clearly dominate stable EVC expression. The alteration of the epigenetic landscape by Tax and other molecular mechanisms such as expression changes of epigenetic modifiers will be elucidated by comprehensive analysis such as a genome-wide ChIP analysis.

In the context of molecular targeting, a new possibility for the HH inhibitor was suggested. Recently, aberrant HH activation and its contribution to cell survival and the cell cycle have been reported in various cancer cells.[11,12] In agreement with other tumors where HH is active, we found that ATL was sensitive against GANT61. This compound can inhibit HH signaling by preventing DNA binding of the GLI family and has few impacts on the viability of healthy CD4+ T cells. We note that we could not confirm the EVC-directed upregulation of common HH target genes such as *Cyclin D1* and *Bcl-2* in ATL models (data not shown). Given that the HH pathway regulates transcription of many genes important for cell fate and many inhibitors against HH cascade have been developed,[16] our findings suggest that pharmacological drugs that can inhibit the HH pathway may be feasible for ATL treatment. Identification of ATL-specific HH target genes will help understanding of the HH roles in survival capability.

In summary, we have identified EVC overexpression as a specific character of ATL and HTLV-1-infected T cells. We have demonstrated the molecular mechanism that overexpressed EVC1 contributes to ATL cell survival. Considering aberrant gene expression associated with cancers, the emerging relationship between epigenetic regulation and the HH pathway provides us with conceptual advance in understanding the broad-acting oncogenic signaling.

Acknowledgments

The authors thank Dr M. Iwanaga and Ms T. Akashi for support and maintenance of JSPFAD and Mr Y. Sasaki for experimental support of the IHC study. The authors also thank Drs H. Miyoshi and A. Miyawaki for providing the Venus-encoding lentivirus vectors and Dr S. Okada for providing the NOJ mice. This work is supported by JSPS KAKENHI Grant Numbers 24790436 (M.Y.) and 23390250 (T.W.), MEXT KAKENHI Grant Number 221S0001 (T.W.), Grant-in-Aid from the Ministry of Health, Labour and Welfare H24-Third Term Cancer-004 (T.W.), and a grant from the Uehara Memorial Foundation (M.Y.).

Disclosure Statement

The authors have no conflict of interest.

References

1 Uchiyama T, Yodoi J, Sagawa K, Takatsuki K, Uchino H. Adult T-cell leukemia: clinical and hematologic features of 16 cases. *Blood* 1977; **50**: 481–92.
2 Poiesz BJ, Ruscetti FW, Gazdar AF, Bunn PA, Minna JD, Gallo RC. Detection and isolation of type C retrovirus particles from fresh and cultured lymphocytes of a patient with cutaneous T-cell lymphoma. *Proc Natl Acad Sci USA* 1980; **77**: 7415–9.
3 Yoshida M, Miyoshi I, Hinuma Y. Isolation and characterization of retrovirus from cell lines of human adult T cell leukemia and its implication in the disease. *Proc Natl Acad Sci USA* 1982; **79**: 2031–5.
4 Tsukasaki K, Utsunomiya A, Fukuda H *et al.* VCAP-AMP-VECP compared with biweekly CHOP for adult T-cell leukemia–lymphoma: Japan Clinical Oncology Group Study JCOG9801. *J Clin Oncol* 2007; **25**: 5458–64.
5 Yamagishi M, Nakano K, Miyake A *et al.* Polycomb-mediated loss of miR-31 activates NIK-dependent NF-κB pathway in adult T cell leukemia and other cancers. *Cancer Cell* 2012; **21**: 121–35.
6 Yamagishi M, Watanabe T. Molecular hallmarks of adult T cell leukemia. *Front Microbiol* 2012; **3**: 334.
7 Grassmann R, Aboud M, Jeang KT. Molecular mechanisms of cellular transformation by HTLV-1 Tax. *Oncogene* 2005; **24**: 5976–85.
8 Hall WW, Fujii M. Deregulation of cell-signaling pathways in HTLV-1 infection. *Oncogene* 2005; **24**: 5965–75.
9 Mori N, Fujii M, Ikeda S *et al.* Constitutive activation of NF-kappaB in primary adult T-cell leukemia cells. *Blood* 1999; **93**: 2360–8.
10 Watanabe M, Ohsugi T, Shoda M *et al.* Dual targeting of transformed and untransformed HTLV-1-infected T cells by DHMEQ, a potent and selective inhibitor of NF-kappaB, as a strategy for chemoprevention and therapy of adult T-cell leukemia. *Blood* 2005; **106**: 2462–71.
11 Low JA, de Sauvage FJ. Clinical experience with Hedgehog pathway inhibitors. *J Clin Oncol* 2010; **28**: 5321–6.
12 Briscoe J, Thérond PP. The mechanisms of Hedgehog signalling and its roles in development and disease. *Nat Rev Mol Cell Biol* 2013; **14**: 416–29.
13 Johnson RL, Rothman AL, Xie J *et al.* Human homolog of patched, a candidate gene for the basal cell nevus syndrome. *Science* 1996; **272**: 1668–71.
14 Dierks C, Grbic J, Zirlik K *et al.* Essential role of stromally induced hedgehog signaling in B-cell malignancies. *Nat Med* 2007; **13**: 944–51.
15 Singh RR, Kim JE, Davuluri Y *et al.* Hedgehog signaling pathway is activated in diffuse large B-cell lymphoma and contributes to tumor cell survival and proliferation. *Leukemia* 2010; **24**: 1025–36.
16 McMillan R, Matsui W. Molecular pathways: the hedgehog signaling pathway in cancer. *Clin Cancer Res* 2012; **18**: 4883–8.
17 Tompson SWJ, Ruiz-Perez VL, Blair HJ *et al.* Sequencing EVC and EVC2 identifies mutations in two-thirds of Ellis-van Creveld syndrome patients. *Hum Genet* 2007; **120**: 663–70.
18 Ruiz-Perez VL, Blair HJ, Rodriguez-Andres ME *et al.* Evc is a positive mediator of Ihh-regulated bone growth that localises at the base of chondrocyte cilia. *Development* 2007; **134**: 2903–12.
19 Dorn KV, Hughes CE, Rohatgi R. A Smoothened-Evc2 complex transduces the Hedgehog signal at primary cilia. *Dev Cell* 2012; **23**: 823–35.
20 Yamamoto K, Ishida T, Nakano K *et al.* SMYD3 interacts with HTLV-1 Tax and regulates subcellular localization of Tax. *Cancer Sci* 2011; **102**: 260–6.
21 Sasaki H, Hui C, Nakafuku M, Kondoh H. A binding site for Gli proteins is essential for HNF-3beta floor plate enhancer activity in transgenics and can respond to Shh *in vitro*. *Development* 1997; **124**: 1313–22.
22 Yamagishi M, Ishida T, Miyake A *et al.* Retroviral delivery of promoter-targeted shRNA induces long-term silencing of HIV-1 transcription. *Microbes Infect* 2009; **11**: 500–8.
23 Miyoshi H, Takahashi M, Gage FH, Verma IM. Stable and efficient gene transfer into the retina using an HIV-based lentiviral vector. *Proc Natl Acad Sci USA* 1997; **94**: 10319–23.

24 Miyoshi H, Blömer U, Takahashi M, Gage FH, Verma IM. Development of a self-inactivating lentivirus vector. *J Virol* 1998; **72**: 8150–7.
25 Kobayashi S, Nakano K, Watanabe E *et al.* CADM1 expression and stepwise downregulation of CD7 are closely associated with clonal expansion of HTLV-I-infected cells in adult T-cell leukemia/lymphoma. *Clin Cancer Res* 2014; **20**: 2851–61.
26 Sasaki D, Imaizumi Y, Hasegawa H *et al.* Overexpression of enhancer of zeste homolog 2 with trimethylation of lysine 27 on histone H3 in adult T-cell leukemia/lymphoma as a target for epigenetic therapy. *Haematologica* 2011; **96**: 712–9.
27 Smith MR, Greene WC. Identification of HTLV-I tax trans-activator mutants exhibiting novel transcriptional phenotypes. *Genes Dev* 1990; **4**: 1875–85.
28 Tsuji T, Sheehy N, Gautier VW, Hayakawa H, Sawa H, Hall WW. The nuclear import of the human T lymphotropic virus type I (HTLV-1) tax protein is carrier- and energy-independent. *J Biol Chem* 2007; **282**: 13875–83.
29 Lauth M, Bergström A, Shimokawa T, Toftgård R. Inhibition of GLI-mediated transcription and tumor cell growth by small-molecule antagonists. *Proc Natl Acad Sci USA* 2007; **104**: 8455–60.
30 Blair HJ, Tompson S, Liu YN *et al.* Evc2 is a positive modulator of Hedgehog signalling that interacts with Evc at the cilia membrane and is also found in the nucleus. *BMC Biol* 2011; **9**: 14.
31 Ego T, Ariumi Y, Shimotohno K. The interaction of HTLV-1 Tax with HDAC1 negatively regulates the viral gene expression. *Oncogene* 2002; **21**: 7241–6.
32 Kamoi K, Yamamoto K, Misawa A *et al.* SUV39H1 interacts with HTLV-1 Tax and abrogates Tax transactivation of HTLV-1 LTR. *Retrovirology* 2006; **3**: 5.

Supporting Information

Additional supporting information may be found in the online version of this article:

Fig. S1. HTLV-1 *HBZ* does not affect EVC expression.

Fig. S2. EVC knockdown reduces ATL cell proliferation.

Methods S1. Including: details of clinical samples; and primer sequences used in the present study.